





DESIGN OF WIRELESS POWER TRANSFER COILS FOR ELECTRIC VEHICLES AND ANALYSING THE COUPLING COEFFICIENT ACCORDING TO THE CHANGING COIL INNER DIAMETER

^{1,*} Yasin AKÜN , ²Abdulsamed TABAK 

^{1,2} Necmettin Erbakan University, Engineering Faculty, Mechatronics Engineering Department, Konya,
TÜRKİYE

¹yasinakun@gmail.com, ²atabak@erbakan.edu.tr

Highlights

- FEM analysis of coupling coefficient based on changing inner diameter of coils
- Wireless power systems classified by transmission distance
- Coil design for WPT done using Maxwell 3D from Ansys Electronics



DESIGN OF WIRELESS POWER TRANSFER COILS FOR ELECTRIC VEHICLES AND ANALYSING THE COUPLING COEFFICIENT ACCORDING TO THE CHANGING COIL INNER DIAMETER

^{1,*} Yasin AKÜN^{id}, ² Abdulsamed TABAK^{id}

^{1,2} Necmettin Erbakan University, Engineering Faculty, Mechatronics Engineering Department, Konya,
TÜRKİYE

¹ yasinakun@gmail.com, ² atabak@erbakan.edu.tr

(Received: 21.05.2025; Accepted in Revised Form: 23.08.2025)

ABSTRACT: The popularity of electric vehicles (EVs) is steadily increasing, and their adoption is becoming more widespread. This growing prevalence has led to increased interest in wireless and contactless charging systems for EVs as alternatives to traditional wired methods. Consequently, it is essential to analyse the factors that affect the efficiency of wireless power transfer (WPT). In WPT systems, a primary coil is installed at the charging station, while a secondary coil is positioned beneath the vehicle. Power transmission occurs due to the magnetic field generated between these two coils. One of the key factors influencing the efficiency of WPT is the coupling coefficient. This study examines the impact of variations in the inner diameters of identically designed primary and secondary coils on the coupling coefficient. The analysis was performed using the ANSYS Electronics – Maxwell 3D simulation tool. The results indicate that increasing the inner diameter of the coils from 50 mm to 300 mm leads to a 69.23% increase in the coupling coefficient. This study offers an original contribution by systematically analysing the impact of varying inner coil diameters on the coupling coefficient in coaxial WPT systems, a topic not yet thoroughly addressed in the existing literature.

Keywords: ANSYS Maxwell 3D, Coil Design, Coupling Coefficient, Electric Vehicles (EVs), Wireless Power Transfer (WPT)

1. INTRODUCTION

A historical examination of automobiles reveals that electric vehicles (EVs) were initially more popular than internal combustion engine (ICE) vehicles. However, in the early 20th century, factors such as falling oil prices and the mass production of the Ford Model T contributed to the growing preference for ICE vehicles. Today, the vast majority of vehicles in use worldwide still rely on traditional internal combustion engines. The fossil fuels consumed by these vehicles are a major contributor to carbon emissions, thereby accelerating global warming [1].

Electric vehicles are widely recognized as a cornerstone of sustainable transportation. Nevertheless, one of the primary challenges hindering their widespread adoption is the lack of practical and accessible charging infrastructure. In this context, wireless charging technology emerges as a promising and innovative solution. This technology enables energy transfer to EVs without the need for physical cable connections, operating on the principle of electromagnetic induction. Specifically, a transmitter coil embedded in the road or parking space transfers energy to a receiver coil mounted beneath the vehicle via an electromagnetic field. As a result, EVs can be charged both while stationary and in motion [2] [3].

Wireless charging not only eliminates the inconvenience of manual cable handling but also significantly enhances the overall user experience. Moreover, the absence of exposed cables contributes to improved aesthetics and safety at charging stations. In urban environments, where vandalism is a concern, this system can help protect the charging infrastructure from damage. Once a vehicle is parked, charging can commence automatically without human intervention. In the future, this technology is expected to evolve into fully automated charging systems integrated with autonomous vehicles [4], [5], [6].

*Corresponding Author: Yasin AKÜN, yasinakun@gmail.com

Wireless power transfer (WPT) has undergone several stages of development and has now reached a maturity level suitable for high-energy-demand applications such as EVs. Despite notable theoretical and practical advancements, its integration with autonomous vehicles represents a critical milestone in the evolution of intelligent and environmentally friendly transportation. Wireless charging is anticipated to fundamentally transform how EVs are powered. With continued research and development, the technology is expected to become more efficient, cost-effective, and widespread. Wireless EV charging represents a significant step toward achieving sustainable transportation goals by offering convenience to users and enabling more efficient utilization of charging infrastructure [7], [8], [9].

As WPT systems continue to advance and become increasingly prevalent—particularly in automotive, medical, and industrial applications—it becomes ever more critical to analyse their complex architectures. Ensuring high performance and stability under varying system parameters is of paramount importance. Numerous studies in the literature have addressed these challenges. For instance, Li and Mi emphasized the importance of achieving a high coupling coefficient (k) and quality factor (Q) to ensure efficient energy transfer [10]. Ankur and Tushar focus on designing multiple circular coil geometries for wireless power transfer in electric vehicles, analysing parameters like coupling coefficient, mutual inductance, and self-inductance [11]. Sample et al. analysed system efficiency under various frequencies, distances, and coil alignment scenarios [12]. Sagar et al. presented a comprehensive review of recent developments in coupling configurations, coil types, compensation techniques, misalignment tolerance, and control strategies [9]. Wageningen and Staring reported that coupling efficiency decreases as misalignment increases and the distance between coils grows [13]. Wen and Zhang investigated the performance of WPT systems using various magnetic materials across different frequency ranges, finding ferrite materials to offer the highest efficiency [14]. A collaborative study on semi-dynamic WPT for autonomous EVs reported a maximum efficiency of 90.8% in static mode and over 85% during dynamic charging [15]. It is possible to see studies in the literature on different coil types, for example Viswanath and Venkata focus on inductively coupled wireless charging systems, specifically using double-D coils. It analyses the coupling coefficient and system performance, optimizing ferrite core dimensions rather than coil inner diameter, achieving a maximum coupling coefficient of 0.2451 with specific dimensions [16]. Another study conducted by Hu et al., an advanced low-power MCRWPT (Magnetic Coupling Resonant Wireless Power Transfer) system with LCC-LCC compensation was designed using a ferrite-nanocrystalline hybrid shielding method and a relay coil, achieving an increase in efficiency from 40.38% to 69.17%. Furthermore, compared to full ferrite shielding, the proposed hybrid method is 63.11% lighter while providing improvements in efficiency, reduction in magnetic leakage, and cost advantages [17]. In the study conducted by Hu et al., a 2.5 kW 400/48 V IPT system was developed for low-voltage, high-current electric mobility applications, featuring an asymmetrical double-sided LCC compensation and passive current balancing. System performance was validated through Ansys Maxwell 3D simulations and MATLAB/PSIM analyses, demonstrating effective current sharing under component mismatch and misalignment conditions [18]. In a low-power WPT application, the use of a bidirectional LCLC topology resulted in an 84.70% reduction in stray electromagnetic fields and a 0.907% increase in power transfer efficiency [19]. Despite these contributions, a limited number of studies explicitly address the effect of inner coil diameter on the coupling coefficient. Ozupak investigated different coil configurations and highlighted that increasing inner diameter can enhance coupling but also introduce spatial constraints [20]. Also, Ozupak emphasized that coil dimensioning must consider not only magnetic performance but also mechanical feasibility within EV chassis layouts [21]. While several review articles [5], [7], [9] provide valuable overviews of WPT technology, many lack a critical analysis of trade-offs such as system size, manufacturability, and electromagnetic compatibility. Most notably, very few publications conduct a dedicated analysis of inner coil diameter as an independent design parameter. The current study fills this gap by systematically investigating how changing the inner diameter affects coupling efficiency using ANSYS Maxwell 3D simulations.

This work contributes to the growing body of literature by offering design insights that specifically

address the geometric trade-offs in coil design for EV applications, providing both theoretical analysis and simulation-based results. Additionally, it benchmarks the obtained results with current state-of-the-art literature to contextualize the impact of inner diameter variation on WPT efficiency.

Much of the existing literature has focused on the impact of coil spacing, winding shapes (e.g., square, circular, double-D coils), and winding diameters on the coupling coefficient. However, there is a limited number of studies investigating the effect of variations in the inner diameters of coils on coupling efficiency [22]. Given that wireless power transfer systems generally exhibit lower efficiency compared to their wired counterparts, it is crucial to consider all design parameters that influence efficiency during the system design process. As the inner diameter of the coil is one of the critical parameters affecting power transfer efficiency and the existing literature lacks a comprehensive analysis on this topic, this study aims to explore this parameter in detail. In this context, we examined circular coils with inner diameters of 50, 100, 150, and 300 mm to determine the optimal design parameters for maximizing coupling efficiency.

Although several studies have focused on coil shape, alignment, or compensation methods in WPT systems, very few have examined how changes in the inner diameter affect performance—especially when other parameters are held constant. This study aims to fill that gap by performing a controlled simulation-based analysis of coupling efficiency across various D_{xi} values. The use of identical coil geometry and materials in all test cases ensures that the results directly isolate the impact of inner diameter, thereby providing new insights for coil optimization in electric vehicles.

2. MATERIAL AND METHODS

WPT systems can be classified based on transmission distance. Since transmission distance is typically a primary consideration in WPT systems, categorizing these systems by distance is significant for guiding the structure and focus of related research. Figure 1 presents the classification of wireless power transfer systems according to transmission distance [23].

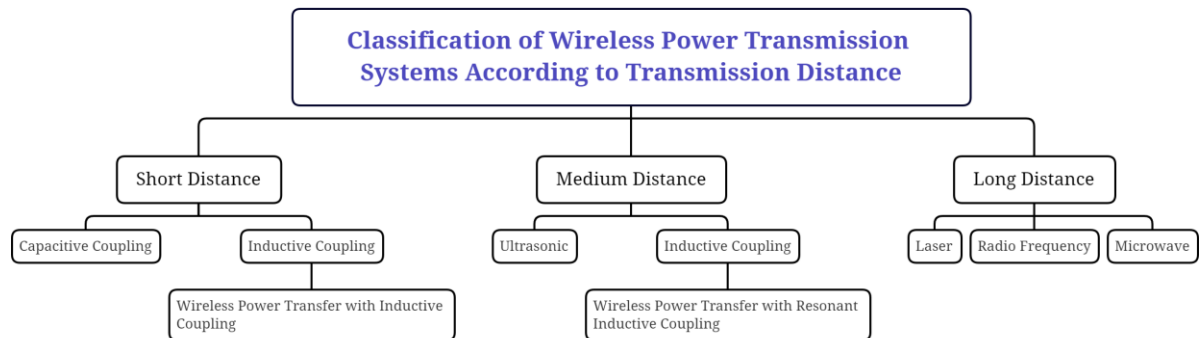


Figure 1. Classification of Wireless Power Transmission Systems Based on Transmission Distance

In the design of WPT systems, passive circuit elements such as capacitors, inductors, and resistors are essential. These components are responsible for providing compensation within the circuit of the WPT system. Compensation is crucial in inductive power transfer systems to enhance power transfer capability, minimize the volt-ampere (VA) rating of the power source, and regulate the circuit's voltage levels as well as the current in the power supply loop [24]. Compensation is implemented independently on both the primary and secondary sides of the system. The level of compensation within the system is evaluated using the quality factor Q_p on the primary side and Q_s on the secondary side. Equations (1) and (2) illustrate the quality factors for the primary and secondary sides, respectively.

$$Q_p = \frac{\omega L_p}{R_i} \quad (1)$$

$$Q_s = \frac{\omega L_s}{R_L} \quad (2)$$

Here, R_L denotes the load resistance, ω represents the angular frequency, L_p is the inductance of the coil on the primary side, and L_s refers to the inductance of the coil on the secondary side [25].

Figure 2 illustrates the four fundamental topologies—series-series, series-parallel, parallel-series, and parallel-parallel—classified based on the configuration of the capacitor within the circuit. Among these methods, studies have identified the series-series topology as the most optimal configuration [26].

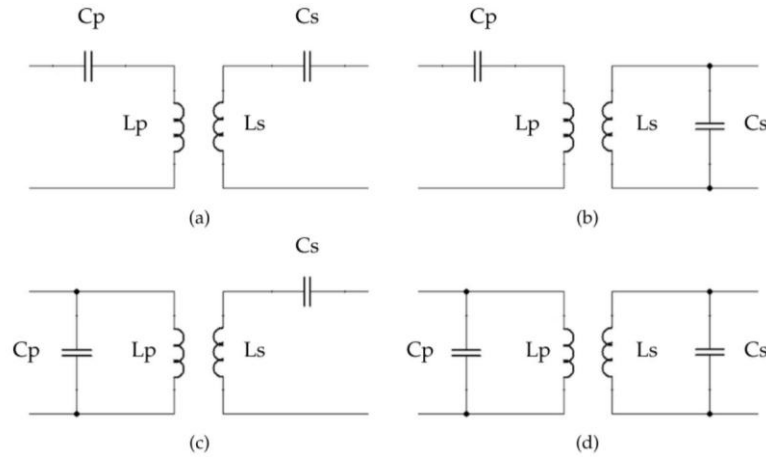


Figure 2. Fundamental compensation topologies. (a) series-series. (b) series-parallel. (c) parallel-series. (d) parallel-parallel.

The coupling effect between the two sides arises when the coils are in mutual interaction. The coupling coefficient is defined as the ratio of the mutual inductance between the coils to the geometric mean of their self-inductances and is expressed within the range of 0 to 1. The self-inductance of the primary coil is denoted as L_p , while the self-inductance of the secondary coil is represented as L_s . The mutual inductance induced in the primary coil due to interaction with the secondary coil is denoted by M_{12} , and the mutual inductance induced in the secondary coil due to interaction with the primary coil is represented as M_{21} . The coupling coefficient between the two coils is expressed by Equation (3) [27].

$$k = \sqrt{\frac{M_{12}M_{21}}{L_b L_i}} \quad (3)$$

If $M_{12} = M_{21} = M$ is taken, when Equation (4) is rearranged, the coupling coefficient is expressed as Equation (4).

$$k = \frac{M}{\sqrt{L_b L_i}} \quad (4)$$

Based on the expression in Equation (4), it can be inferred that an increase in the inductance value leads to an increase in the coupling coefficient. Mutual inductance was formulated by Maxwell through Equation (5). The mutual inductance of two coaxial circular loops, with radius A and a , separated by a certain distance, is obtained by evaluating the Neumann integral over the perimeters of both loops. The variables F and E , which appear in the formulation as the complete elliptic integrals of the first and second kinds, respectively, depend on the parameter k [27].

$$M = \mu_0 \sqrt{Aa} \left[\left(\frac{2}{k} - k \right) F(k) - \frac{2}{k} E(k) \right] \text{ [Henry]} \quad (5)$$

Equation (6) represents the integral variable k [27].

$$k = \frac{\sqrt{r_1^2 - r_2^2}}{r_1} \quad (6)$$

The efficiency of power transfer between the coils is expressed Equation (7) as a function of the coupling coefficient k and the quality factors Q_p and Q_s [25].

$$\eta_e = \frac{k^2 Q_p Q_s}{1 + Q_p^2 + k^2 Q_p Q_s} \quad (7)$$

Circular coils were selected in this study due to their well-known symmetrical magnetic field distribution, which enhances alignment tolerance and efficiency in wireless power transfer systems. Compared to other shapes such as rectangular or double-D coils, circular configurations offer simpler analytical modelling, uniform mutual inductance, and ease of fabrication. These characteristics make them particularly suitable for initial performance analysis in simulation-based design studies like this one.

2.1. Ansys Electronics-Maxwell 3D

Ansys Electronics Maxwell 3D is an advanced finite element analysis software used for electromagnetic field simulations. It is employed in the design, optimization, and analysis of electromagnetic components such as electric motors, transformers, magnetic actuators, sensors, and wireless power transfer (WPT) systems. The software supports static, time-dependent (transient), and frequency-domain (AC) analyses. It enables the investigation of the effects of electromagnetic fields on devices and allows for accurate magnetic analysis in complex geometries and materials. Calculations such as inductance, magnetic flux density, magnetic saturation, and leakage flux can also be performed. Ansys Maxwell 3D is part of the Ansys Electronics suite and is optimized for low-frequency electromagnetic analyses. By computing the distribution of electric and magnetic fields, it provides a means to evaluate and improve device performance. Since WPT systems transmit energy from one point to another using electromagnetic fields, Ansys Maxwell 3D is well-suited for the design, optimization, and performance analysis of such systems. For these reasons, Ansys Electronics was chosen for this study. Figure 3 represents the example of study using Ansys Maxwell.

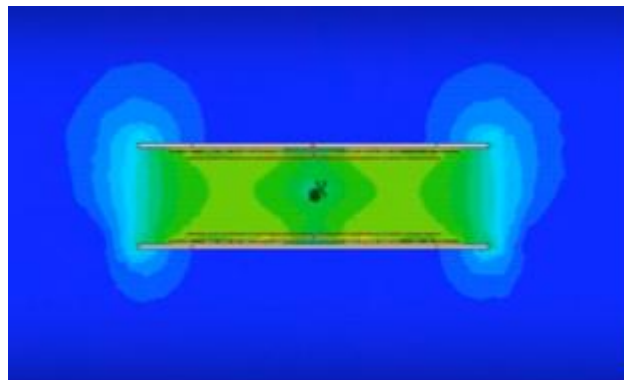


Figure 3. A sample of finite element analysis study using Ansys Maxwell.

To ensure the accuracy and stability of the simulation results, a mesh convergence analysis was performed using ANSYS Maxwell 3D's adaptive meshing feature. The mesh refinement per pass was set to 30%, with a minimum of 1 pass and 1 converged pass required for validation. The adaptive mesh

setup was further configured to allow a maximum of 2 passes, and the simulation was set to stop when the percentage error dropped below 1%. These parameters ensured that the solution reached numerical stability while minimizing simulation time. By controlling the refinement process and error threshold, the reliability of the coupling coefficient results was maintained throughout all coil configurations.

3. RESULTS AND DISCUSSION

In this study, coil designs for wireless power transfer were developed using Maxwell 3D, a tool within the Ansys Electronics suite. Analyses were conducted based on variations in the inner diameters of the coils, which were expected to influence the coupling coefficient. The wireless power transfer system was designed to transfer power from a stationary primary part to a vehicle-mounted secondary part using the resonant inductive coupling method. To perform the analysis using the finite element method, the primary and secondary components were modelled in Ansys Maxwell 3D, with the necessary parameters defined to simulate under desired conditions. The designed primary and secondary coils are identical and coaxial. In both sections, a ferrite core was incorporated to enhance inductance, and an aluminium plate was added to minimize magnetic flux leakage. Figure 4 illustrates the designed plate, while the properties of the plate used in the Ansys simulations are provided in Table 1.

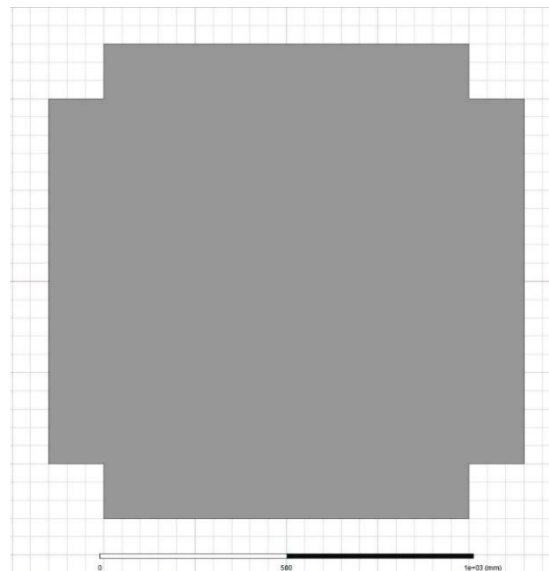


Figure 4. Aluminium plate design.

Table 1. Features of the plate designed in Ansys

Features	Descriptions
Material	Aluminum
Material Color	Gray
Z Size	5 mm
X Size	1300 mm
Y Size	1300 mm
Relative Permittivity	1
Relative Permeability	1.000021
Bulk Conductivity	38000000 siemens/m
Mass Density	2689 kg/m ³

Figure 5 illustrates the designed ferrite. The material properties of the ferrite used in the Ansys analyses are presented in Table 2.

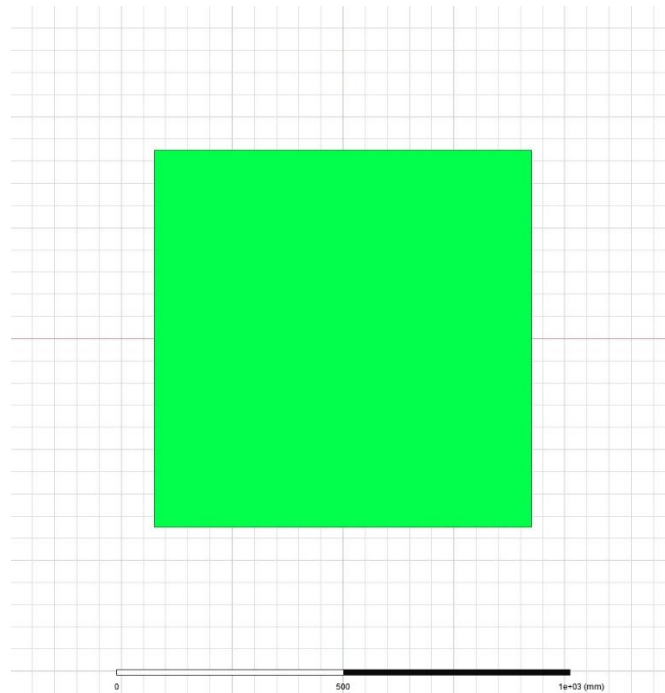


Figure 5. Ferrite design.

Table 2. Features of the ferrite designed in Ansys

Features	Descriptions
Material	FDK6H40
Material Color	Green
Z Size	4 mm
X Size	850 mm
Y Size	850 mm
Relative Permittivity	1
Relative Permeability	2400
Bulk Conductivity	0 siemens/m

Figure 6 presents the designed coil. The properties of the coil used in the Ansys analyses are provided in Table 3. The number of turns and the internal length of the coil are not included in the table, as they vary depending on the specific analysis.

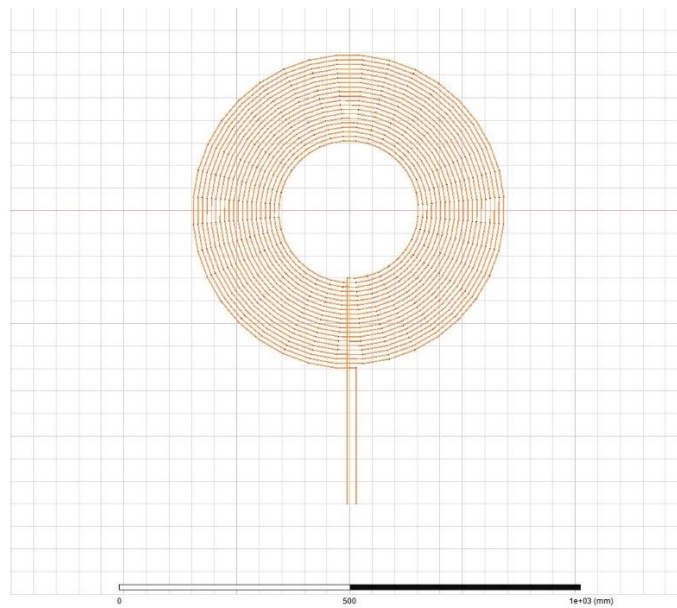


Figure 6. Circular coil design.

Table 3. Features of the coil designed in Ansys

Features	Descriptions
Material	Copper
Material Color	Orange
Coil Type	Stranded
Cross Section Area	5.2 mm ²
Radius Change	10mm
Length	1300 mm
Number of Conductors	96
Current	31.73 A
Relative Permittivity	1
Relative Permeability	0.999991
Bulk Conductivity	58000000 siemens/m
Mass Density	8933 kg/m ³

Table 4 presents the design parameters that were kept constant throughout the analyses.

Table 4. Shows the system parameters that held constant in the analyses for the designed WPT system.

Parameters	Values
Resonance frequency (f_0)	85kHz
Power	7.3kW
Supply Voltage	230V
Distance Between Primary and Secondary Coils	130 mm
Number of Coil Turns $N_{1,2}$	20

Within the scope of this study, the inner diameter length of the D_{xi} coil is defined as a design variable. The effect of variations in D_{xi} on the coupling coefficient was investigated by analysing the

coupling coefficients of coil pairs with different D_{xi} lengths. Figure 7 shows the illustration of the inner diameter variable (D_{xi}), Figure 8 (a-b) and 9 (a-b) show designs with D_{xi} values of 50 mm, 100 mm, 150 mm, and 300 mm.

Globally, EVs are categorized into different segments based on their size and specifications. The selected D_{xi} values were determined in relation to four EV segments: A, B, C, and D. One of the main reasons for choosing a maximum D_{xi} value of 300 mm is that, when other design parameters are held constant, increasing the inner diameter of the coil significantly enlarges the overall system size, leading to both physical and design-related challenges. The selection of inner coil diameters (D_{xi} = 50 mm, 100 mm, 150 mm, 300 mm) was based on typical chassis dimensions across standard EV segments. For example:

Segment A (compact city EVs) like the Renault Zoe (~4.1 m length, ~1.7 m width) typically have under-body packaging spaces aligning with coil diameters up to ~100 mm without structural interference. Segment B–C (mid-size EVs) such as the Volkswagen ID.3 (~4.3 m × 1.8 m) and Tesla Model 3 (~4.7 m × 2.0 m) offer clearance to support coil diameters of ~150 mm within battery tray areas while maintaining motor/inverter spacing. Segment D (executive EVs) like the BMW i4 (~4.8 m × 1.85 m) offer larger flat under-body floorpan areas, enabling coil diameters up to ~300 mm without compromising chassis integrity or ground clearance. These outer limits were cross-referenced with public EV chassis floorpan designs and underbody clearance specs, confirming that studied coil sizes are not only theoretically relevant but also practical in current EV platforms. This contextualization strengthens the justification for chosen D_{xi} values.

In particular, a D_{xi} value exceeding 300 mm would substantially increase the winding area of both the primary and secondary coils, making it difficult to control the physical dimensions. The manufacturing and assembly of large-diameter coils would complicate the mechanical integration of the system and potentially cause the vehicle to exceed its current design constraints.

In the integration of WPT systems into electric vehicles, there are spatial limitations for the secondary coil of the wireless charging system, which is typically mounted under the chassis. Exceeding these spatial constraints would necessitate a redesign of the vehicle's underbody and could adversely affect critical parameters such as aerodynamics and centre of gravity.

Therefore, the selected D_{xi} values were determined to ensure compatibility with electric vehicle design standards while facilitating the physical integration of the system.

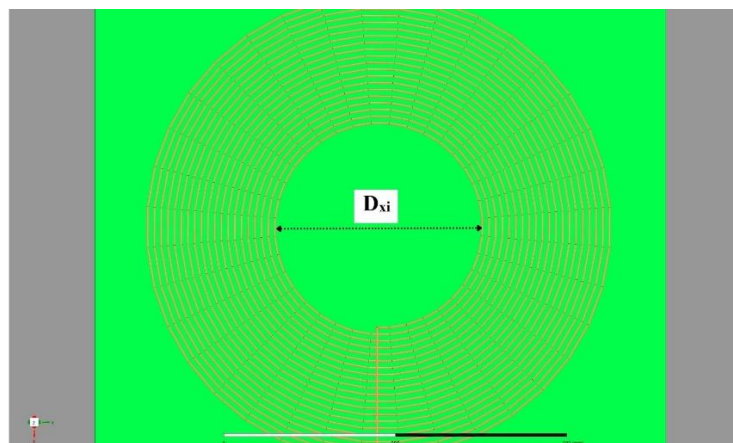


Figure 7. Illustration of the inner diameter variable (D_{xi}) in a coil with circular topology.

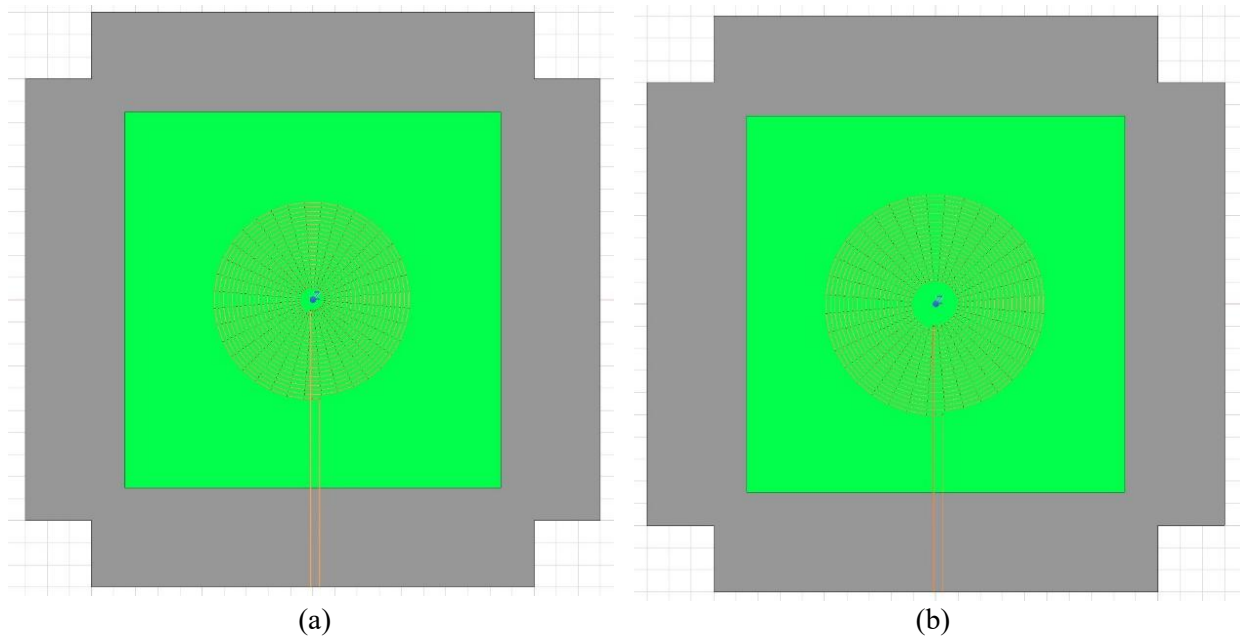


Figure 8. Circular primary-side coil with an inner length of (a) $D_{xi} = 50$ mm and (b) $D_{xi} = 100$ mm.

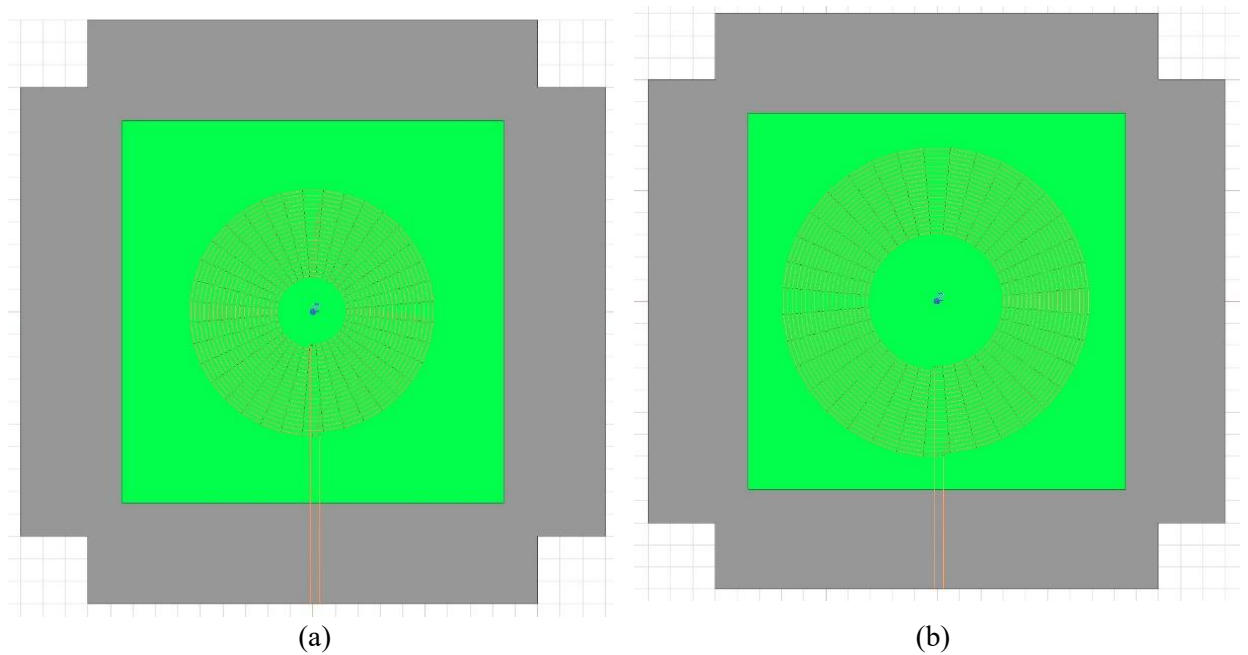


Figure 9. Circular primary-side coil with an inner length of (a) $D_{xi} = 150$ mm and (b) $D_{xi} = 300$ mm.

Figure 10 shows the primary and secondary coils positioned coaxially and symmetrically with respect to each other.

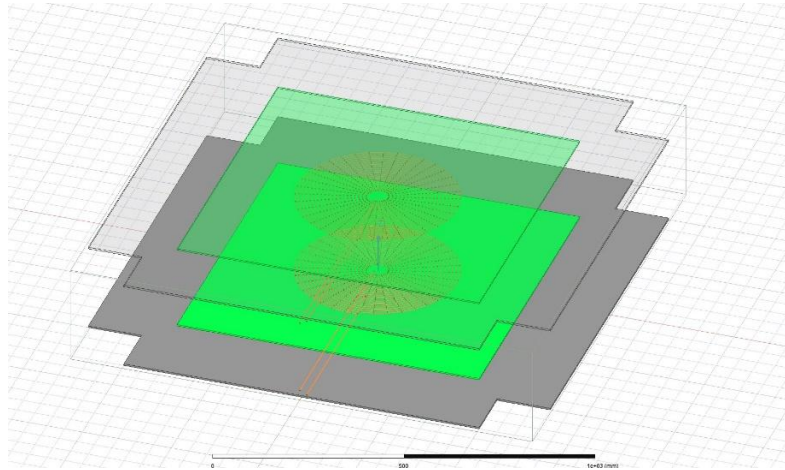


Figure 10. Design of symmetrical and coaxially aligned primary and secondary coils with identical geometries.

The D_{xi} values of the opposing coils are identical. The D_{xi} parameter, which represents the inner diameter of the coils, was defined at 50 mm, 100 mm, 150 mm, and 300 mm, and analyses were conducted accordingly. In all analyses, the number of turns in the coils was kept equal. The coupling coefficients obtained within these specified D_{xi} ranges are presented in Table 5. Accordingly, the coupling coefficient increased from 0.36 at $D_{xi} = 50$ mm to 0.41 at 100 mm, 0.45 at 150 mm, and 0.52 at 300 mm. Thus, increasing D_{xi} from 50 mm to 300 mm resulted in an approximate 69.23% improvement in the coupling coefficient.

Table 5. Variation of the coupling coefficient with respect to coil inner diameter in the WPT system

D_{xi} (mm)	Coupling Coefficient
50	0.36
100	0.41
150	0.45
300	0.52

Based on Table 5, which illustrates the effect of the increase in coil inner diameter on the coupling coefficient, it can be concluded that systems designed with larger coil inner diameters will achieve higher coupling. As the coupling coefficient increases, the energy transfer between the primary and secondary coils becomes more efficient. Since the increase in the coil inner diameter also leads to a larger overall coil diameter, larger coils create a broader magnetic field, which induces a higher magnetic flux in the opposing coil. Considering that electric vehicle chassis sizes will vary according to their segments, selecting larger coil inner diameters for the system design of larger-segment electric vehicles will enhance the system's efficiency. For wireless power transfer systems designed for vehicles in different segments, it is necessary to optimize the coil inner diameter values.

Table 6. Comparison of coupling coefficient values reported in recent WPT studies and this study

Study	Coil Configuration	Coupling Coefficient	Key Features
This Study	Circular, coaxial coils ($D_{xi} = 50\text{--}300\text{ mm}$)	0.36 – 0.52	Inner diameter effect analysed systematically
Sundari & Sakthi (2022) [28]	Spiral/rectangular coils, 95 kHz	~0.2635	Simulated mutual inductance 9.16 μH , rectangular vs spiral
Hu et al. (2025) [29]	Hybrid ferrite-nanocrystalline shielding	0.45 – 0.52	LCC-LCC compensation, dynamic operation
Viswanath & Venkata (2024) [16]	Ferrite-based double-D coils	0.2451	Compact design, ferrite dimension tuning
Lo & Juwono & Wong & Chew (2022) [30]	Circular coils, outer $\Phi 330\text{--}400\text{ mm}$	0.273 \rightarrow 0.321 with ferrite & Al	Larger diameter improves coupling; shielding better performance

Table 6 presents a comparison between the coupling coefficients obtained in this study and those reported in similar recent research. The values obtained in our simulation (ranging from 0.36 to 0.52) are consistent with results from advanced configurations such as optimized double-D coils and hybrid shielding systems. While some studies, like Viswanath & Venkata (2024), report lower coupling due to compact design constraints, others achieve comparable results through complex coil geometries or shielding methods. Unlike previous works, our study isolates the inner diameter parameter while keeping all other design variables constant, providing a focused and novel analysis.

Although detailed flux distribution visuals are not presented in this version of the study, magnetic field behaviour was observed during simulations in ANSYS Maxwell 3D through the analysis of magnetic flux density and vector fields. The primary and secondary coils exhibited symmetric and concentric field patterns, consistent with the coaxial geometry. In future versions, flux distribution figures will be included to provide additional insight into field uniformity and potential leakage areas.

In this study, each simulation scenario for different D_{xi} values was conducted as a single run due to computational resource limitations and the deterministic nature of the simulation model. As the system was modelled under controlled and ideal conditions using finite element analysis (FEA) in ANSYS Maxwell 3D, the output values (such as the coupling coefficient) are inherently stable and reproducible across identical runs. For this reason, statistical measures such as standard deviation or multiple trials were not considered necessary. Nevertheless, in future work, a more comprehensive statistical analysis could be included to assess variability under non-ideal or dynamic operating conditions.

Although numerous studies have investigated the effects of coil geometry, alignment, and compensation topologies on wireless power transfer efficiency, no existing research was found that specifically analyses the impact of varying inner coil diameters D_{xi} using the same design and simulation parameters. Due to the absence of comparable studies with matching D_{xi} configurations, a direct one-to-one comparison of the coupling coefficient values was not feasible. As a result, the results of this study are presented as original findings that address a gap in the current WPT literature. Future studies may benefit from extending this analysis to benchmark it against emerging research with similar design setups.

The ferrite and aluminium plate thicknesses used in this study were chosen to minimize magnetic flux leakage and enhance coupling efficiency under ideal simulation conditions. However, it is acknowledged that such material dimensions may not be optimal in terms of weight and integration within real-world electric vehicle systems. Future work will focus on evaluating the impact of thinner ferrite and aluminium structures to strike a balance between electromagnetic performance and mechanical feasibility, especially for lightweight and compact EV applications.

4. CONCLUSIONS

The demand for wireless charging has emerged in order to charge electric vehicles in a comfortable and practical way. Especially with the widespread adoption of autonomous vehicle technology, wireless charging systems will become even more inevitable. This study presents an investigation of the coupling coefficient, which affects the efficiency of wireless power transfer in electric vehicles, based on changes in the coil inner diameter. In the study, identical and coaxial primary and secondary coils are used in the wireless power transfer system to provide energy transmission for electric vehicles. Each analysis includes evaluations with four different D_{xi} values representing the coil inner diameter. By selecting different values for the coil inner diameters, the effectiveness of power transfer was examined. The results show that increasing the inner diameters of the identically designed coaxial coil pair significantly increases the coupling coefficient. The coupling coefficients for the coils with inner diameters of 50 mm, 100 mm, 150 mm, and 300 mm are 0.36, 0.41, 0.45, and 0.52, respectively. This highlights the importance of considering not only the distance between coils, the coil wire structure, and design differences but also the inner radius of the coils as a key design parameter. It is suggested that different D_{xi} values should be optimized for electric vehicles in different segments. For small vehicles in segment A, coils with smaller D_{xi} values may be preferred, while for larger vehicles in segments B, C, and D, coils with larger D_{xi} values could be used. The study is expected to make a significant contribution as a study examining design parameters to improve the efficiency of wireless power transfer systems. However, the practical feasibility of the system must also be considered. As the coil sizes increase, it is essential to analyse how well the system integrates with other vehicle components and the impact on the overall performance. Future studies will focus on investigating the effect of this inner diameter on the coupling coefficient in different coil designs and its relationship with the cable cross-section.

Future research could explore the impact of alternative coil geometries, such as rectangular, hexagonal, or double-D topologies, on coupling efficiency under varying inner diameters. Additionally, parametric optimization methods could be employed to determine the optimal balance between coil size, number of turns, and material selection. The integration of wireless coils with vehicle suspension, battery tray layouts, and shielding strategies may also be investigated to improve compatibility with EV architectures. While this study acknowledges that increasing coil diameter may pose spatial and mechanical integration challenges in EVs, a detailed engineering assessment was beyond its scope. In future work, finite element modelling of the full vehicle underbody—including structural supports, cooling systems, and electromagnetic shielding—could be used to evaluate how coil placement interacts with critical vehicle systems. This would strengthen the practical applicability of the proposed coil configurations.

Declaration of Ethical Standards

The authors declare that all ethical guidelines including authorship, citation, data reporting, and publishing original research are followed.

Credit Authorship Contribution Statement

Yasin AKÜN: Investigation, Methodology, Software, Writing-original draft, Validation. Abdulsamed TABAK: Investigation, Methodology, Software, Writing-review & editing, Validation.

Declaration of Competing Interest

The authors declare that there is no conflict of interest.

Funding / Acknowledgements

This research received no specific grant from any funding agency in the public, commercial, or not-for-profit sectors.

Data Availability

Not applicable.

REFERENCES

- [1] H. Uçarol *et al.*, "Hibrid ve Elektrikli Araçlar Ulaşımında enerji Verimliliği için Bir Alternatif," *TÜBİTAK Marmara Araştırma Merk. Enerj. Enstitüsü*, pp. 170–174, 2009.
- [2] Y. Yang, J. Cui, and X. Cui, "Design and analysis of magnetic coils for optimizing the coupling coefficient in an electric vehicle wireless power transfer system," *Energies*, vol. 13, no. 6, 2020, doi: 10.3390/en13164143.
- [3] X. Zhang, Z. Yuan, Q. Yang, Y. Li, J. Zhu, and Y. Li, "Coil Design and Efficiency Analysis for Dynamic Wireless Charging System for Electric Vehicles," *IEEE Trans. Magn.*, vol. 52, no. 7, pp. 1–4, 2016, doi: 10.1109/TMAG.2016.2529682.
- [4] E. Aydin, M. T. Aydemir, A. Aksoz, M. El Baghdadi, and O. Hegazy, "Inductive Power Transfer for Electric Vehicle Charging Applications: A Comprehensive Review," *Energies*, vol. 15, no. 14, 2022, doi: 10.3390/en15144962.
- [5] A. Mahesh, B. Chokkalingam, and L. Mihet-Popa, "Inductive Wireless Power Transfer Charging for Electric Vehicles-A Review," *IEEE Access*, vol. 9, pp. 137667–137713, 2021, doi: 10.1109/ACCESS.2021.3116678.
- [6] H. Feng, R. Tavakoli, O. C. Onar, and Z. Pantic, "Advances in High-Power Wireless Charging Systems: Overview and Design Considerations," *IEEE Trans. Transp. Electr.*, vol. 6, no. 3, pp. 886–919, 2020, doi: 10.1109/TTE.2020.3012543.
- [7] S. Shen, Z. Zhang, Y. Wu, R. Wang, and Z. Liang, "Modelless Prediction of Variable Coupling Effect for Multiple-Load Wireless Power Transfer," *IEEE Trans. Magn.*, vol. 58, no. 2, pp. 1–5, 2022, doi: 10.1109/TMAG.2021.3089784.
- [8] Z. Zhang, H. Pang, A. Georgiadis, and C. Cecati, "Wireless Power Transfer - An Overview," *IEEE Trans. Ind. Electron.*, vol. 66, no. 2, pp. 1044–1058, 2019, doi: 10.1109/TIE.2018.2835378.
- [9] A. Sagar *et al.*, "A Comprehensive Review of the Recent Development of Wireless Power Transfer Technologies for Electric Vehicle Charging Systems," *IEEE Access*, vol. 11, pp. 83703–83751, 2023, doi: 10.1109/ACCESS.2023.3300475.
- [10] S. Li and C. C. Mi, "Wireless power transfer for electric vehicle applications," *IEEE J. Emerg. Sel. Top. Power Electron.*, vol. 3, no. 1, pp. 4–17, 2015, doi: 10.1109/JESTPE.2014.2319453.
- [11] A. Yadav and T. K. Bera, "Design and Analysis of Circular Coil Geometries for Wireless Power Transfer in Electric Vehicles The Effect of Multiple Coils at Primary and Secondary Sides," *Proc. - 2nd Int. Conf. Power Electron. Energy, ICPEE 2023*, pp. 1–6, 2023, doi: 10.1109/ICPEE54198.2023.10060651.
- [12] A. P. Sample, D. A. Meyer, and J. R. Smith, "Analysis, experimental results, and range adaptation of magnetically coupled resonators for wireless power transfer," *IEEE Trans. Ind. Electron.*, vol. 58, no. 2, pp. 544–554, 2011, doi: 10.1109/TIE.2010.2046002.
- [13] D. van Wageningen and T. Staring, "The Qi wireless power standard," *Proc. EPE-PEMC 2010 - 14th Int. Power Electron. Motion Control Conf.*, pp. S15-25-S15-32, 2010, doi: 10.1109/EPEPEMC.2010.5606673.
- [14] H. Wen and C. Zhang, "Investigation on transmission efficiency for magnetic materials in a wireless power transfer system," in *Proc. Int. Conf. Power Electron. Drive Syst. (PEDS)*, Sydney, NSW, Australia, 2015, pp. 249–253, doi: 10.1109/PEDS.2015.7203423.

- [15] C. H. Lee, G. Jung, K. Al Hosani, B. Song, D. K. Seo, and D. Cho, "Wireless power transfer system for an autonomous electric vehicle," *2020 IEEE Wirel. Power Transf. Conf. WPTC 2020*, pp. 467–470, 2020, doi: 10.1109/WPTC48563.2020.9295631.
- [16] V. Chakibanda and V. L. N. Komanapalli, "Coil Parameter Analysis for Inductively Coupled Wireless Charging for Electric Vehicles," *Vehicles*, vol. 6, no. 1, pp. 468–483, 2024, doi: 10.3390/vehicles6010021.
- [17] Y. Hu, T. Heng, T. Zhang, W. Zhou, and Q. Chen, "An Improved Magnetic Coupling Resonant Wireless Power Transfer System Based on Ferrite-Nanocrystalline Hybrid Shielding Method," *Int. J. Circuit Theory Appl.*, pp. 1–14, 2024, doi: 10.1002/cta.4280.
- [18] M. T. Tran, S. Thekkan, H. Polat, D. D. Tran, M. El Baghdadi, and O. Hegazy, "Inductive Wireless Power Transfer Systems for Low-Voltage and High-Current Electric Mobility Applications: Review and Design Example," *Energies*, vol. 16, no. 7, 2023, doi: 10.3390/en16072953.
- [19] Y. Li, Y. Ying, K. Xie, and S. Pan, "A Dual-Sided LCLC Topology for AGV Wireless Charging System With Low Leakage EMF," *IEEE Trans. Electromagn. Compat.*, vol. 65, no. 3, pp. 643–654, 2023, doi: 10.1109/TEMC.2023.3263906.
- [20] Y. Özüpak, "Analysis of the Parameters Affecting the Efficiency of the Wireless Power Transmission System Designed for New Generation Electric Vehicles," *Int. J. Automot. Technol.*, vol. 24, no. 6, pp. 1675–1680, 2023, doi: 10.1007/s12239-023-0135-1.
- [21] Y. Özüpak, "Analysis and experimental verification of efficiency parameters affecting inductively coupled wireless power transfer systems," *Heliyon*, vol. 10, no. 5, 2024, doi: 10.1016/j.heliyon.2024.e27420.
- [22] Y. Yang, M. El Baghdadi, Y. Lan, Y. Benomar, J. Van Mierlo, and O. Hegazy, "Design methodology, modeling, and comparative study of wireless power transfer systems for electric vehicles," *Energies*, vol. 11, no. 7, 2018, doi: 10.3390/en11071716.
- [23] M. Çiçek, S. Balcı, and K. Sabancı, "A Comparative Performance Analysis of Wireless Power Transfer with Parametric Simulation Approach," *Kastamonu Univ. J. Eng. Sci.*, vol. 9, no. 1, pp. 17–32, 2023, doi: 10.55385/kastamonujes.1298700.
- [24] W. Zhang, S. C. Wong, C. K. Tse, and Q. Chen, "Design for efficiency optimization and voltage controllability of series-series compensated inductive power transfer systems," *IEEE Trans. Power Electron.*, vol. 29, no. 1, pp. 191–200, 2014, doi: 10.1109/TPEL.2013.2249112.
- [25] K. N. Mude and K. Aditya, "Comprehensive review and analysis of two-element resonant compensation topologies for wireless inductive power transfer systems," *Chinese J. Electr. Eng.*, vol. 5, no. 2, pp. 14–31, 2019, doi: 10.23919/CJEE.2019.000008.
- [26] A. S. Yilmaz and U. Kızıldağ, "Wireless Charging Systems In Electric Vehicles and A Sample System Investigation," *Adıyaman Üniversitesi Mühendislik Bilim. Derg.*, vol. 8, pp. 209–224, 2021.
- [27] G. Uzun, "Kablosuz Enerji İletimi," M.S. Thesis, *Graduate School of Natural and Applied Sciences, Ondokuz Mayıs Üniversitesi*, Samsun, Türkiye, 2012.
- [28] B. Sakthi and P. Sundari, "Design of coil parameters for inductive type wireless power transfer system in electric vehicles," *Int. J. Energy Res.*, vol. 46, May 2022, doi: 10.1002/er.8016.
- [29] Y. Hu, T. Heng, T. Zhang, W. Zhou, and Q. Chen, "An Improved Magnetic Coupling Resonant Wireless Power Transfer System Based on Ferrite-Nanocrystalline Hybrid Shielding Method," *Int. J. Circuit Theory Appl.*, vol. 53, no. 6, pp. 3592–3605, Jun. 2025, doi: <https://doi.org/10.1002/cta.4280>.
- [30] D. Lo, F. Juwono, W. K., and I. Chew, "A study on transmission coil parameters of wireless power transfer for electric vehicles," *Serbian J. Electr. Eng.*, vol. 19, pp. 129–145, Jan. 2022, doi: 10.2298/SJEE2202129L.